



Published in final edited form as:

Brain Res. 2021 March 15; 1755: 147263. doi:10.1016/j.brainres.2020.147263.

Accelerated brain aging in chronic low back pain

Gary Z Yu^{1,*}, Maria Ly^{2,*}, Helmet T. Karim³, Nishita Muppidi¹, Howard J. Aizenstein^{1,3}, James W. Ibinson^{4,5}

¹Department of Bioengineering, University of Pittsburgh, Pittsburgh, PA, USA

²Center for Neuroscience, University of Pittsburgh, Pittsburgh, PA, USA

³Department of Psychiatry, University of Pittsburgh, Pittsburgh, PA, USA

⁴Department of Anesthesiology, University of Pittsburgh, Pittsburgh, PA, USA

⁵VA Pittsburgh Health System, Pittsburgh, PA, USA

Abstract

Chronic low back pain (CLBP) is a leading cause of disability and is associated with neurodegenerative changes in brain structure. These changes lead to impairments in cognitive function and are consistent with those seen in aging, suggesting an accelerated aging pattern. In this study we assessed this using machine-learning estimated brain age (BA) as a holistic metric of morphometric changes associated with aging. Structural imaging data from 31 non-depressed CLBP patients and 32 healthy controls from the Pain and Interoception Imaging Network were included. Using our previously developed algorithm, we estimated BA per individual based on grey matter density. We then conducted multivariable linear modeling for effects of group, chronological age, and their interaction on BA. We also performed two voxel-wise analyses comparing grey matter density between CLBP and control individuals and the association between grey matter density and BA. There was an interaction between CLBP and greater chronological age on BA such that the discrepancy in BA between healthy and CLBP individuals was greater for older individuals. In CLBP individuals, BA was not associated with sex, current level of pain, duration of CLBP, or mild to moderate depressive symptoms. CLBP individuals had lower cerebellar grey matter density compared to healthy individuals. Brain age was associated with

Corresponding Author: James W. Ibinson, MD, PhD, UPMC Montefiore, 3459 Fifth Avenue, Pittsburgh, PA 15213, Tel: (412) 647-3147, ibinsonjw@upmc.edu.

* Gary Z. Yu and Maria Ly serve as co-first authors on this manuscript

Author Contributions:

Data Collection: Data used in preparation of this article/manuscript/abstract were acquired from the Pain and Interoception Imaging Network — PAIN Repository (painrepository.org). PAIN Repository investigators may have provided data but not otherwise participated in the analysis or preparation of this report. The PAIN repository is funded by the National Institutes of Health (NIDA, NCCAM) under award number R01AT007137.

Conceptualization: GZY, ML, HTK, JI, HJA

Analysis and Interpretation of Results: GZY, ML, HTK, JI, NM, HJA

Drafting of Manuscript: GZY, ML, HTK, JI, HJA

Critical Revision of Manuscript: GZY, ML, HTK, JI, NM, HJA

All authors discussed the results and commented on the manuscript.

Declarations of interest: none

Publisher's Disclaimer: This is a PDF file of an unedited manuscript that has been accepted for publication. As a service to our customers we are providing this early version of the manuscript. The manuscript will undergo copyediting, typesetting, and review of the resulting proof before it is published in its final form. Please note that during the production process errors may be discovered which could affect the content, and all legal disclaimers that apply to the journal pertain.

lower gray matter density in numerous brain regions. CLBP was associated with greater BA, which was more profound in later life. BA as a holistic metric was sensitive to differences in gray matter density in numerous regions which eluded direct comparison between groups.

Keywords

chronic low back pain; aging; machine learning; structural neuroimaging

1. Introduction

Low back pain (LBP) is the leading cause of disability worldwide (James et al., 2017). Most adults are likely to suffer from LBP during some point in their lives, and the number of years lost to disability from this condition has increased by 54% since 1990 (Hartvigsen et al., 2018). LBP is highly prevalent and challenging to manage clinically. In most cases, the specific source of pain cannot be identified, resulting in classification as non-specific LBP (Buchbinder et al., 2018). In addition, LBP is often accompanied by and exacerbates medical comorbidities, requiring additional care for poorer treatment response (Foster et al., 2018). LBP is highly persistent, with approximately two-thirds of patients still reporting pain after twelve months (Meucci et al., 2015).

There is a mounting body of literature suggesting that chronic LBP (CLBP) may have detrimental effects on brain structure. These alterations in brain structure may result in symptoms that extend beyond nociception, leading to impairment in attention, mental flexibility, language skills, and emotional decision making (Buckalew et al., 2010; Ivo et al., 2013; Malfliet et al., 2017; Wand et al., 2011).

Specifically, CLBP has been associated with changes in gray matter density (GMD) in multiple regions, namely the prefrontal cortex, thalamus, brainstem, corpus callosum, and total gray matter volume, although the direction of these changes has been conflicting in various studies (Apkarian et al., 2004; Buckalew et al., 2010; Ivo et al., 2013; Kregel et al., 2015; Schmidt-Wilcke et al., 2006). Past studies have shown that these differences in gray matter are normalized following treatment (Seminowicz et al., 2011; Seminowicz et al., 2013).

Brain age is a machine-learning driven approach of assessing global gray matter density of an individual compared against age-matched healthy peers as a holistic metric of brain health and structural integrity. Given the complex patterns of brain morphometric changes associated with the aging process between different individuals, brain age serves as a holistic aggregate metric of numerous regional structural changes (Eavani et al., 2018). As such, brain age may be sensitive to patterns and impacts of various pathologic insults beyond traditional voxel-based morphometric analyses and is especially suitable for analysis of age-related pathologies given its innate capacity to define structural changes in terms of accelerated aging. We have demonstrated this in our previously developed and validated brain age model in the context of Alzheimer's disease, and a recent application of BA to general chronic pain has also shown significant discrepancies between healthy individuals

and individuals with chronic pain (Ly et al., 2019; Cruz-Almeida et al., 2019). However, whether these differences hold true specifically in individuals with CLBP is yet unexplored.

Therefore, in this study we applied our BA prediction model to a cohort of CLBP patients without depression. Since it has been suggested that chronic pain may result in “accelerated aging” of the brain, we hypothesized that CLBP patients would present with higher BA for any given chronologic age compared to healthy controls. In addition, we investigated the association between BA and factors of CLBP duration and pain severity at the time of imaging for the CLBP group. Finally, we conducted a more traditional voxel-wise analysis to identify regions where GMD was associated with group (adjusting for sex, age, and age squared) as well as a voxel-wise analysis to identify specific brain regions correlated with BA (adjusting for sex, age, and age squared).

2. Results:

The model predicted age accurately in CLBP and healthy individuals with $r = 0.45$, $R^2 = 0.20$, and $MAE = 5.1$. Compared to the healthy control group, the CLBP group was not significantly different in participant age or sex, but had significantly greater current pain, pain duration, and depressive symptoms (Table 1).

Overall, the multivariable linear model predicted BA and explained 32% of the variance in BA ($r(62) = 0.57$, $R^2 = 0.32$, $RMSE = 3.46$). Group moderated the association between chronological age and BA (corrected model – $F(5,62) = 6.93$, $p < 0.001$, Table 2). There was a significant interaction effect between CLBP status and chronological age on predicted BA ($p = 0.031$, Table 2, Figure 1). Sex was not associated with BA and did not moderate the association between chronological age and BA. Within the CLBP group, none of the following factors were directly associated with BA: sex, current pain, pain duration, and depressive symptoms (Table 3).

Adjusting for sex, age, and age squared, we found that HC showed greater GMD in the cerebellum compared to CLBP, but lower GMD in the left cuneus and superior occipital gyrus (table 4, figure 2). Adjusting for sex, age, and age squared, we found that greater BA residual (which has sex, age, and age squared regressed out – i.e., is independent of these factors) was associated with lower GMD in a number of regions throughout the brain including the cingulate, amygdala, visual cortex, cerebellum, frontal cortex, temporal gyrus, hippocampus/parahippocampus, insula, motor/sensory cortex, and putamen (table 5, figure 3).

3. Discussion and conclusions:

In this study we sought to apply a machine learning-based BA prediction model to a CLBP cohort without depression with age and sex matched healthy controls. Given the various documented deleterious effects of CLBP on brain structure, we hypothesized that the CLBP group would have older predicted BA for a given chronological age compared to the HC group. Our results supported this hypothesis, as CLBP participants showed an additional 0.15 years (approximately 1.8 months) in predicted BA per chronological year of life

compared to their healthy counterparts. In other terms, CLBP participants appeared to age an additional 1.8 months per year of life compared to their healthy counterparts.

The greater slope of the CLBP group's BA to chronological age trendline against the HC line (and therefore a greater discrepancy between the two at greater ages) supports previous models regarding CLBP as being associated with accelerated aging. Many of the changes in brain structure seen in CLBP, such as lower GMD in the prefrontal cortex, thalamus, and brainstem, are also seen in the natural aging process (Apkarian et al., 2004; Ivo et al., 2013; Kregel et al., 2015). As greater BA was significantly associated with lower GMD in numerous regions, we may assume that the discrepancies between the healthy and CLBP groups may be partially ascribed to lower GMD in said regions. Notably, these included the prefrontal cortex, parietal cortex, brainstem, and limbic regions involved in pain interoception including the hippocampus, amygdala, and insula.

In addition, due to the greater slope of the CLBP trendline, the discrepancy in brain age between the two groups would theoretically be larger at greater chronological ages, although this was not a longitudinal study. This possibly suggests that older adults with CLBP are at risk for the greatest brain morphometric changes given their longitudinal pain burden. As emphasized by previous studies, there are numerous significant differences in brain structure and function in older adults with CLBP compared to their healthy counterparts (Buckalew et al., 2010). Especially relevant from Buckalew et al. (2010) is that changes in brain structure associated with late-onset depression were seen even in non-depressed CLBP participants, suggesting that an absence of depression does not preclude the structural changes and increased vulnerability to psychiatric comorbidities. Previous literature has also shown that degenerative brain changes in older CLBP patients are distinct from younger CLBP patients, and that older adults are unable to effectively respond to pain due to age-related changes in areas of central pain regulation (Apkarian et al., 2004; Karp et al., 2008). However, because the confidence intervals for trendlines at younger ages overlapped, these differences may not be as robust in younger individuals.

We found that sex, depressive symptoms, duration of pain, and current pain were not significantly associated with brain age, suggesting an alternative driving factor not encompassed by these variables. One aspect to consider is that total duration of pain and current pain level may be imperfect quantifiers of a patient's trajectory with CLBP. Not only is it possible for pain intensity to change over time, the duration in which a patient experiences higher levels of pain may also be a contributory factor for the activation and possible enhanced response of various pain-related brain regions (Flor et al., 2001; Wand et al., 2011). Previous literature has also suggested that both normal and pathologic structural brain changes themselves may contribute toward a patient's experience of CLBP due to impairment of descending inhibition, implicating a bidirectional relationship between structural brain changes and chronic pain (Karp et al., 2008). All these factors suggest that the trajectory of CLBP and its relationship to brain changes are more complex than may be characterized by measurements of only duration and pain at one instance (Flor et al., 2001).

Additionally, while BDI scores were taken as a measure of depressive symptoms in participants, most scores for CLBP participants were below the clinical threshold for major

depressive disorder (BDI = 16). Although there is an extensive relationship between CLBP and depression, with overlap in their underlying neurobiology and impact on brain structure, our results suggest that there are also significant effects of CLBP on brain structure in the absence of Major Depressive Disorder (Gerhart et al., 2018; Hung et al., 2015; Karp et al., 2012). However, two participants excluded as outliers had BDI scores of 17 and 19, with brain ages 15 and 21 years older than their chronological ages, respectively. A general positive trend between BDI scores in the major depressive disorder levels and greater brain aging in CLBP patients is suggested by the few participants which meet the clinical BDI threshold in the present study; however, further investigation of CLBP patients with major depressive disorder would be needed to draw a more definitive conclusion regarding brain age.

Healthy control participants also showed significantly greater GMD in the cerebellum compared to CLBP participants. This result reinforces previous findings demonstrating significantly reduced gray matter volume of the cerebellum in participants with lumbar disk herniation, a common etiology of CLBP (Luchtmann et al., 2014). With regards to general nociception, previous work has suggested that the cerebellum has a modulatory role in nociceptive processing including voluntary motor inhibition during pain and anticipation of pain (Fields, 2000; Ploghaus et al., 1999). In addition to these findings, lower integrity of the cerebellum was also associated with impaired proprioception in individuals with CLBP, also implicating poor postural control as a possible underlying mechanism of non-specific low back pain (Pijnenburg et al., 2014).

While the CLBP participants also demonstrated greater GMD in the superior occipital gyrus and left cuneus, the significant regions were much smaller and less significant compared to the cerebellar findings. Although the occipital gyrus and precuneus have been shown to have increased activation in visualization of pain in individuals with LBP, our findings may also be more sample-specific given our cohort size.

When assessing the contribution of lower GMD to greater brain age (independent of age and sex), many more regions were significantly associated with brain age in addition to the cerebellum (figure 3). Given the widespread nature of GMD contributions to brain age, our results of greater brain age in CLBP individuals support previous findings emphasizing heterogenic global patterns of structural reorganization in chronic pain (Baliki et al., 2011).

The complex, multi-regional associations between decreased GMD and greater BA also highlight the strength of machine learning-based brain age over previous voxel-based morphometric analyses which directly compare between groups using pre-determined region-of-interest analysis, which may not be sensitive to these heterogenic patterns of structural brain changes. As in our study, where a voxel-based comparison of GMD between healthy and CLBP groups only showed significant differences in the cerebellum, actual structural differences associated with greater brain aging were much more complex and nuanced to detect. This further reinforces previously proposed arguments for the merits of machine learning-based brain age given the difficulties of integrating these heterogenic patterns of structural change present in the aging process into a unified metric (Eavani et al., 2018). In further support of this, a recent study of chronic pain and the discrepancy between

predicted brain age and actual age has also shown significantly greater brain age in chronic pain participants compared to healthy participants, suggesting these findings are not limited to CLBP (Cruz-Almeida et al., 2019).

The main limitations of this study include the lack of complementary parameters including interventions for pain such as opioid medications and non-pharmacologic therapies, psychological function, and somatosensory function, as well as limited sample sizes for CLBP and HC participants and the cross-sectional nature of the data. The main limitations of this study are the limited sample sizes for CLBP and HC participants, as well as its cross-sectional nature. Given that this is one of the first studies to show this association in a relatively small sample, it is important to replicate this study and extend these findings by understanding what factors may contribute to this association. Conclusions regarding trends in brain age would be strengthened by a longitudinal analysis with multiple instances of participant imaging to construct trajectories with the development and treatment of CLBP. Additional measures of both pain intensity and duration at multiple time points would also allow for more sophisticated measures of a cumulative pain burden. A limitation of the brain age model used is its holistic mode of analysis of overall GMD. In addition, the training set of the brain age model was not specifically screened for CLBP status in its participants. Therefore, the predicted brain age is not generated against a healthy control population, but rather a general, mixed population. A potential direction of future investigation may be to delineate the contributions of specific brain regions to accelerated aging.

In this study we have demonstrated that brain age prediction using a machine-learning based model shows accelerated brain aging in individuals with CLBP. In addition, we have demonstrated that brain aging is significantly correlated with lower gray matter densities of numerous brain regions in further support of brain age as an aggregate metric that is sensitive to the complex heterogenic patterns of structural differences in aging.

4. Experimental Procedure:

4.1 Study Participants:

This study included data from 63 participants, with 31 having CLBP and 32 healthy controls (HCs), from the Pain and Interoception Imaging Network. Further study details including inclusion and exclusion criteria may be found at the repository website (<https://www.painrepository.org/repositories/>).

4.2 Data Collected:

CLBP duration was self-assessed in years. The visual analog pain scale was used to assess pain on the day of the MRI scan. Depressive symptoms were self-scored using the Beck Depression Inventory (Beck et al., 1996).

4.3 MRI Data Collection:

All scanning was conducted at the Northwestern University Feinberg School of Medicine on a 3T Siemens Trio TIM research-dedicated scanner (Erlangen, Germany) with an 8-channel head coil. An axial whole brain (1mm³ isotropic) T1-weighted sequence (magnetization

prepared rapid gradient echo, MPRAGE) was collected (TR = 2300 ms, TE = 3.43 ms, TI = 900 ms, FA = 9°) with a field of view 256 × 256 with 160 slices.

4.4 MR processing:

All processing was conducted in SPM12 (<https://www.fil.ion.ucl.ac.uk/spm/software/spm12/>). Structural MRI scans skull signal had been manually removed for de-identification. After bias correction, we conducted segmentation into three tissues: gray matter, white matter, and cerebrospinal fluid. We then used the nonlinear DARTEL (fast diffeomorphic registration) algorithm to register images to the Montreal Neurological Institute (MNI) space then generated a template for this cohort, and then smoothed with a Gaussian smoothing kernel with FWHM of 4 mm (typically 2–4 times that of the native resolution) (Ashburner, 2007). This process generates a GMD map – a factor associated with both gray matter volume and cortical thickness. Since individual structural images need to be registered to the MNI space brain, for participants that have a thick cortical gray matter and large cortical volumes these are in a sense ‘squeezed’ to fit onto the standard brain – these participants have a high GMD (i.e., more gray matter in a smaller space). On the other hand, for participants that have thin cortical gray matter and small cortical volumes these are instead ‘expanded’ resulting in lower GMD. This measure accounts for differences in head size as they are all registered to a single template. Participants with larger heads, volumes, and thickness compared to the template have to be shrunk in order to fit and therefore have greater gray matter density.

4.5 Brain Age Model and Estimation:

We have previously developed a BA estimation algorithm that estimated chronological age from GMD maps (Ly et al., 2019). Additional details regarding the model and databases used in the model training set may be found in the supplement of Ly et al. The model training set did not contain any of the HC or CLBP scans used in this study. In brief, the training set includes 757 images of healthy individuals from the ADNI, Information eXtraction from Images (IXI), and OASIS-3 cohorts. Inclusion criteria included age from 20–85, normal cognitive function, negative beta-amyloid status, and no history of psychosis or neurologic disorders. Gray matter density maps were mean-centered and then a similarity kernel was computed by estimating the dot product between every pair of participants (resulting in an NxN matrix). This was input into a Gaussian Processes Regression. BA for each participant in the CLBP and HC groups was calculated using our algorithm. This involved no new training of the model.

4.6 Statistical Analysis:

All statistical analyses were conducted in JMP Pro 14.1.0 (SAS Institute Inc., 2018). Outliers were identified as values outside 1.5 interquartile range for age or having an absolute studentized residual of predicted BA greater than 3.5. As a result, three participants in the CLBP group and two in the healthy controls (HC) group were not included for statistical modeling. To test for the effect of CLBP on the association between chronological age and predicted BA, a multivariable linear regression was used. We also tested if sex moderated this association, as sex has been a distinguishing factor in the etiology, prevalence, and risk of disability from CLBP (DePalma et al., 2012; Dixon and Gatchel,

1999; Munce and Stewart, 2007). Additionally, due to possible interactions of sub-clinical depressive symptoms with CLBP, we tested if pain duration in years, current pain (VAS), or depressive symptoms (as characterized by the Beck Depression Inventory) moderated the association between chronological age and predicted BA specifically within the CLBP group.

Additionally, we conducted two voxel-wise analyses using SnPM13 (statistical non-parametric mapping toolbox, <http://warwick.ac.uk/snpm>) (Nichols and Holmes, 2002). For all voxel-wise analyses, we used permutation testing (10,000 permutations) to compute non-parametric p-values and adjusted for multiple comparisons by controlling the cluster-wise family-wise error (FWE) rate at $p < 0.05$ (cluster-forming threshold at $p < 0.001$). To identify differences in GMD between groups, we first conducted an independent t-test on the gray matter density maps between CLBP and HC adjusting for sex, age (centered), and age (centered) squared – this aligns with a more traditional approach for identifying differences between groups. To identify which region's GMD would correlate with BA, we first conducted a regression between BA and sex, age (centered), and age (centered) squared ($BA \sim \text{sex} + \text{age} + \text{age}^2$) and extracted the residual of this regression as variance in BA not explained by sex or age – we call this the BA residual. We then conducted a voxel-wise analysis between GMD and BA residual adjusting for sex, age (centered), and age (centered) squared. This helps identify which regions in this sample are correlated with variance in BA that was not correlated to sex or age.

Acknowledgements:

Additional acknowledgements on data sharing for this project may be found in the Supplement. Data used in preparation of this manuscript were acquired from the Pain and Interoception Imaging Network — PAIN Repository (painrepository.org). PAIN Repository investigators may have provided data but not otherwise participated in the analysis of preparation of this report. The PAIN repository is funded by the National Institutes of Health (NIDA, NCCAM) under award number R01AT007137.

Funding sources:

This study was supported by funding from NIMH T32MH019986, ML was supported by T32AG021885, T32AG055381. The Pain and Interoception Imaging Network repository is funded by the National Institutes of Health (NIDA, NCCAM) under award number R01AT007137.

Abbreviations:

LBP	low back pain
CLBP	chronic low back pain
GMD	gray matter density
BA	brain age

References:

- Apkarian AV, et al., 2004. Chronic back pain is associated with decreased prefrontal and thalamic gray matter density. *J Neurosci.* 24, 10410–5. [PubMed: 15548656]
- Ashburner J, 2007. A fast diffeomorphic image registration algorithm. *Neuroimage.* 38, 95–113. [PubMed: 17761438]

- Baliki MN, et al., 2011. Brain morphological signatures for chronic pain. *PLoS one*, 6(10), e26010. [PubMed: 22022493]
- Beck AT, Steer RA, Brown GK, 1996. Beck depression inventory-II. *San Antonio*. 78, 490–498.
- Buchbinder R, et al., 2018. Low back pain: a call for action. *The Lancet*. 391, 2384–2388.
- Buckalew N, et al., 2010. Differences in brain structure and function in older adults with self-reported disabling and nondisabling chronic low back pain. 11, 1183–1197.
- Cruz-Almeida Y, et al., 2019. Chronic pain is associated with a brain aging biomarker in community-dwelling older adults. *Pain*. 160, 1119–1130. [PubMed: 31009418]
- DePalma MJ, Ketchum JM, Saullo TR, 2012. Multivariable analyses of the relationships between age, gender, and body mass index and the source of chronic low back pain. *Pain Medicine*. 13, 498–506. [PubMed: 22390231]
- Dixon AN, Gatchel RJ, 1999. Gender and parental status as predictors of chronic low back pain disability: a prospective study. *Journal of Occupational Rehabilitation*. 9, 195–200.
- Eavani H, et al., 2018. Heterogeneity of structural and functional imaging patterns of advanced brain aging revealed via machine learning methods. *Neurobiology of aging*, 71, 41–50. [PubMed: 30077821]
- Fields HL, 2000. Pain modulation: expectation, opioid analgesia and virtual pain. *Prog. Brain Res*. 122, 245–253. [PubMed: 10737063]
- Flor H, et al., 2001. Effect of sensory discrimination training on cortical reorganisation and phantom limb pain. 357, 1763–1764.
- Foster NE, et al., 2018. Prevention and treatment of low back pain: evidence, challenges, and promising directions. *The Lancet*. 391, 2368–2383.
- Gerhart JJ, et al., 2018. Variability in negative emotions among individuals with chronic low back pain: relationships with pain and function. *Pain*. 159, 342–350. [PubMed: 29140926]
- Hartvigsen J, et al., 2018. What low back pain is and why we need to pay attention. *The Lancet*. 391, 2356–2367.
- Hung CI, Liu CY, Fu TS, 2015. Depression: An important factor associated with disability among patients with chronic low back pain. *Int J Psychiatry Med*. 49, 187–98. [PubMed: 25930736]
- Ivo R, et al., 2013. Brain structural and psychometric alterations in chronic low back pain. *Eur Spine J*. 22, 1958–64. [PubMed: 23392554]
- James SL, et al., 2018. Global, regional, and national incidence, prevalence, and years lived with disability for 354 diseases and injuries for 195 countries and territories, 1990–2017: a systematic analysis for the Global Burden of Disease Study 2017. *The Lancet*, 392(10159), 1789–1858.
- Karp J, et al., 2008. Advances in understanding the mechanisms and management of persistent pain in older adults. *British journal of anaesthesia*. 101, 111–120. [PubMed: 18487247]
- Karp JF, et al., 2012. Addressing both depression and pain in late life: the methodology of the ADAPT study. 13, 405–418.
- Kregel J, et al., 2015. Structural and functional brain abnormalities in chronic low back pain: A systematic review. *Semin Arthritis Rheum*. 45, 229–37. [PubMed: 26092329]
- Luchtman M, et al., 2014. Structural brain alterations in patients with lumbar disc herniation: a preliminary study. *PLoS One*, 9(3), e90816. [PubMed: 24595036]
- Ly M, et al., 2019. Improving brain age prediction models: incorporation of amyloid status in Alzheimer's disease. *Neurobiol Aging*.
- Malfliet A, et al., 2017. Brain changes associated with cognitive and emotional factors in chronic pain: a systematic review. *European Journal of Pain*. 21, 769–786. [PubMed: 28146315]
- Meucci RD, Fassa AG, Faria NM, 2015. Prevalence of chronic low back pain: systematic review. *Rev Saude Publica*. 49.
- Munce SE, Stewart DE, 2007. Gender differences in depression and chronic pain conditions in a national epidemiologic survey. *Psychosomatics*. 48, 394–399. [PubMed: 17878497]
- Nichols TE, Holmes AP., 2002. Nonparametric permutation tests for functional neuroimaging: a primer with examples. *Hum Brain Mapp*. 15:1–25. [PubMed: 11747097]

- Pijnenburg M, et al., 2014. Microstructural integrity of the superior cerebellar peduncle is associated with an impaired proprioceptive weighting capacity in individuals with non-specific low back pain. *PLoS One*, 9(6), e100666. [PubMed: 24949796]
- Ploghaus A, et al., 1999. Dissociating pain from its anticipation in the human brain. *Science* 284, 1979–1981 [PubMed: 10373114]
- Schmidt-Wilcke T, et al., 2006. Affective components and intensity of pain correlate with structural differences in gray matter in chronic back pain patients. *Pain*. 125, 89–97. [PubMed: 16750298]
- Seminowicz DA, et al., 2011. Effective treatment of chronic low back pain in humans reverses abnormal brain anatomy and function. *J Neurosci*. 31, 7540–50. [PubMed: 21593339]
- Seminowicz DA, et al., 2013. Cognitive-behavioral therapy increases prefrontal cortex gray matter in patients with chronic pain. *J Pain*. 14, 1573–84. [PubMed: 24135432]
- Wand BM, et al., 2011. Cortical changes in chronic low back pain: current state of the art and implications for clinical practice. *Man Ther*. 16, 15–20. [PubMed: 20655796]

Highlights:

- Chronic low back pain was associated with greater brain age over chronological age
- Discrepancies between groups for brain age were greatest at older ages
- Individuals with chronic low back pain had lower cerebellar gray matter density
- Higher brain age was linked with a widespread pattern of lower gray matter density
- Brain age may serve as an aggregate measure of holistic gray matter changes

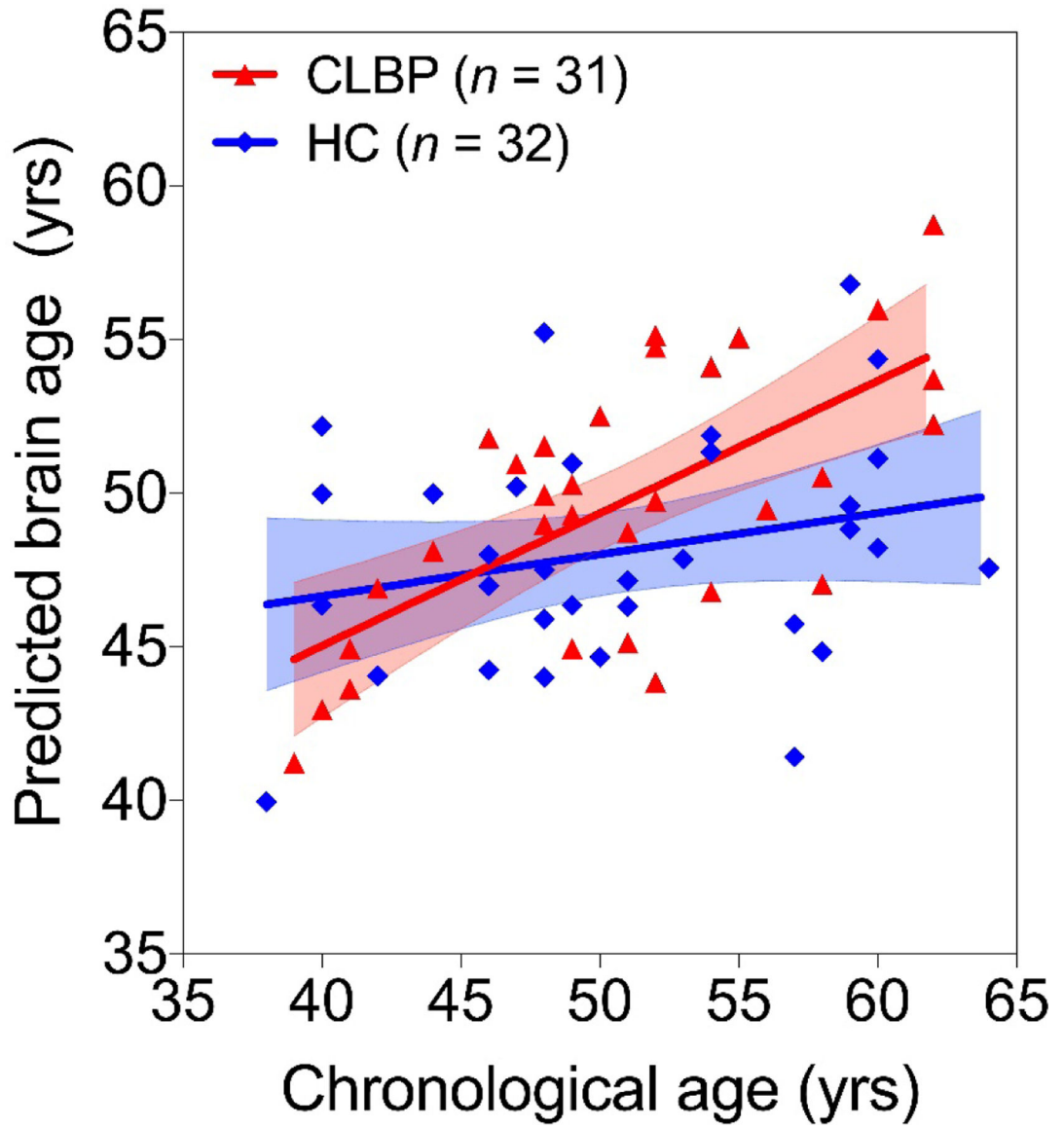


Figure 1:
 CLBP is associated with greater brain age over chronological age - Association between chronological age and predicted brain age in healthy controls (HC, blue) and those with CLBP (red) are shown. Trendlines and 95% confidence intervals (shaded areas) are plotted as well. The CLBP group showed a significantly steeper trend of brain age increases over chronological age representative of a discrepancy in aging exacerbated over the lifespan.

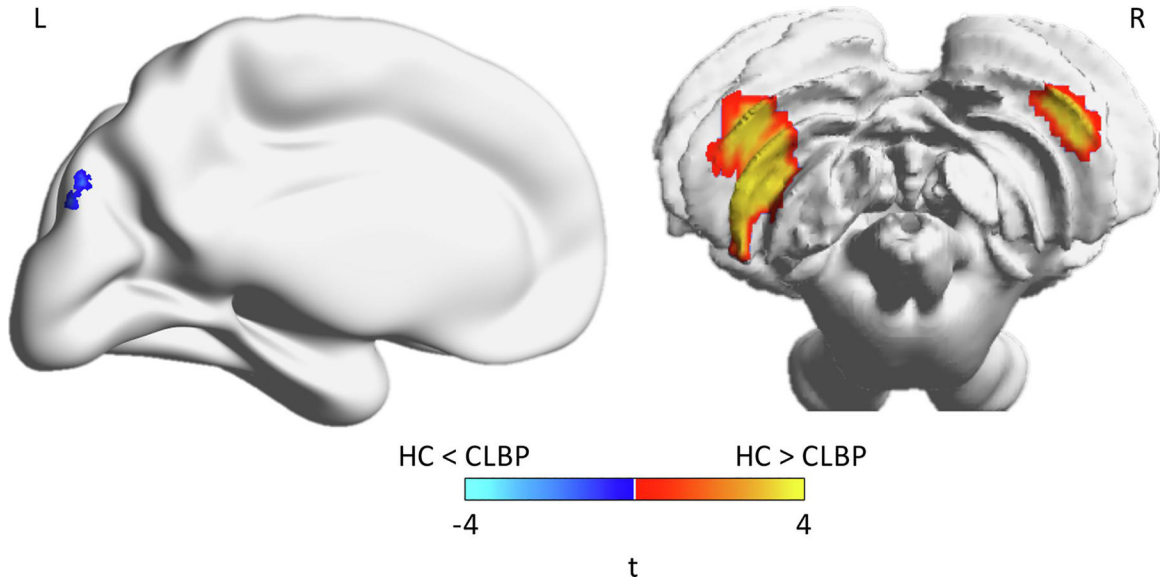


Figure 2: Individuals with CLBP have lower gray matter density - Regions showing significant differences in gray matter density between HC and CLBP (corrected for multiple comparisons). Independent t-test values are plotted on the brain, where cooler colors indicate HC < CLBP while warmer colors indicate HC > CLBP. Brains are plotted using BrainNet Viewer. Note that the cerebellum is shown in radiological view (left-right flipped).

Author Manuscript

Author Manuscript

Author Manuscript

Author Manuscript

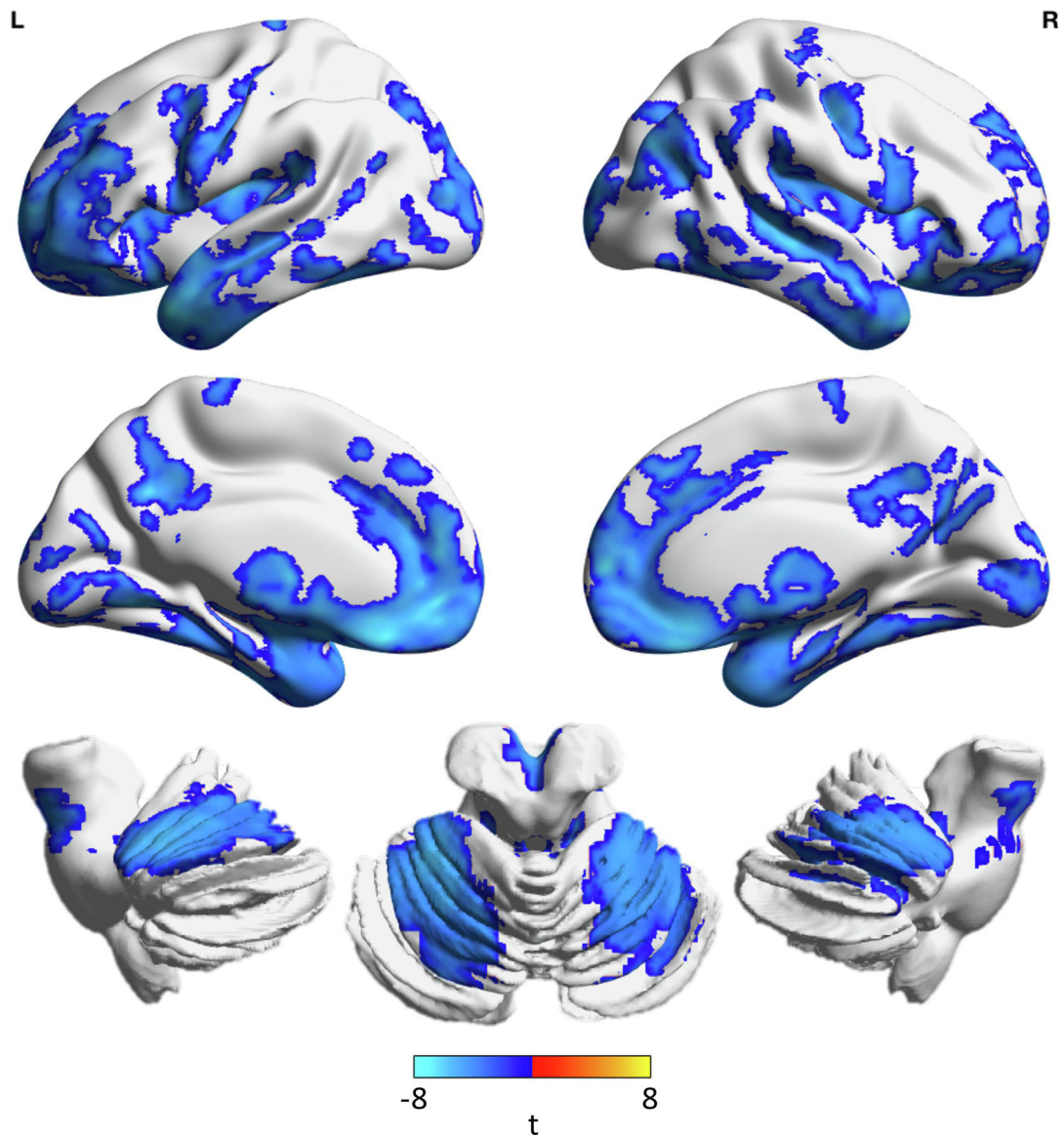


Figure 3:

Greater brain age is associated with lower gray matter density in numerous regions - Regions showing significant association between gray matter density and brain age residual (regressed out sex, age (centered), and age (centered) squared), corrected for multiple comparisons, are shown. Colors indicate the t-value for the regression between gray matter density and brain age residual while adjusting for sex, age (centered), and age (centered) squared. Cooler colors indicate that lower gray matter density is associated with greater brain age (no regions in the opposite direction). Brains are plotted using BrainNet Viewer.

Table 1:

Demographic information and differences between experimental groups are shown. CLBP – Chronic low back pain; HC – healthy controls; VAS – Visual analog scale for pain; BDI – Beck Depression Inventory.

	CLBP (<i>n</i> = 31)	HC (<i>n</i> = 32)	<i>t</i> or χ^2 (df)	<i>p</i> -value
Chronological Age (years)	50.7 (6.5)	50.8 (7.1)	<i>t</i> (62)=0.04	0.967
Sex (% Female)	45.2	43.8	χ^2 (1)=0.01	0.910
Current Pain (VAS)	6.7 (1.8)	0 (0)	<i>t</i> (62)=21.3	<0.001
Pain Duration (years)	16.3 (11.7)	0 (0)	<i>t</i> (62)=7.9	<0.001
BDI	5.5 (5.2)	1.6 (2.7)	<i>t</i> (62)=3.8	<0.001

Table 2:

Statistical results for multivariable linear regression model testing the effect of group on the association between chronological age and predicted brain age. The dependent variable was brain age and the healthy control group was used as reference.

	β with 95% confidence interval			<i>t</i> -statistic	<i>p</i> -value
	β	Lower Bound	Upper Bound		
Intercept	48.393	47.493	49.292	107.72	<0.001*
Chronological Age	0.283	0.152	0.414	4.32	<0.001*
Female sex	-0.68	-1.559	0.199	-1.55	0.127
CLBP	0.789	-0.085	1.662	1.81	0.076
CLBP * Chronological Age	0.145	0.014	0.276	2.22	0.031*

Table 3:

Statistical results for multivariable linear regression model testing the association between the difference between brain and chronological ages and factors of sex, current pain, pain duration, and depressive symptoms for the CLBP group. VAS – Visual analog scale for pain; BDI – Beck Depression Inventory.

	β 95% CI			<i>t</i> -statistic	<i>p</i> -value
	β	Lower Bound	Upper Bound		
Intercept	0.537	-7.260	8.336	0.14	0.888
Sex [F]	-0.300	-2.384	1.783	-0.30	0.769
Current Pain (VAS)	-0.036	-1.334	1.262	-0.06	0.954
Pain Duration (years)	-0.064	-0.265	0.137	-0.65	0.520
BDI	-0.063	-0.526	0.401	-0.28	0.782

Table 4:

Regions showing significant differences in gray matter density between HC and CLBP voxel-wise (corrected for multiple comparisons). Region descriptions are based on AAL3 atlas. The effect column describes the direction of difference. The cluster size and maximum t-value (representing the independent t-test) for the clusters as well as the location of the maximum are reported. Note that there are three significant clusters, however a cluster can have multiple labels, which are indented.

Description	Effect	Cluster Size (# Voxels)	t-value max	MNI coordinate (x, y, z)
Right Cerebellum VIII	HC > CLBP	218	3.7	38, -44, -56
Right Cerebellum VIIb	HC > CLBP	78	4.1	32, -72, -50
Left Cerebellum VIII	HC > CLBP	499	4	-32, -54, -58
Left Cerebellum VIIb	HC > CLBP	94	4.2	-34, -68, -50
Left Cuneus	HC < CLBP	85	-4.8	-2, -90, 38
Left Superior Occipital	HC < CLBP	79	-5.6	-10, -86, 46

Table 5:

Regions showing significant association between gray matter and brain age residual (regress out sex, age (center) and age (center) squared) voxel-wise (corrected for multiple comparisons) – this adjusted for sex, age (centered), and age (centered) squared. Region descriptions are based on AAL3 atlas. Negative values indicate that greater brain age is associated with lower gray matter density (no positive values). The cluster size and maximum t-value (representing the t-value for a regression) for the clusters as well as the location of the maximum are reported. Note that there are three significant clusters, however a cluster can have multiple labels, which are indented.

Description	Cluster Size (# Voxels)	t-value max	MNI coordinate (x, y, z)
Left ACC presubiculum	369	-6.5	-8, 44, 0
Right ACC presubiculum	263	-5.5	8, 50, 12
Left ACC subiculum	92	-5.9	-2, 30, -10
Right ACC subiculum	65	-4.7	6, 34, -8
Left ACC supracallosal	275	-6.1	-6, 36, 24
Right ACC supracallosal	88	-4.7	10, 36, 16
Left Amygdala	194	-5.1	-22, 2, -18
Right Amygdala	175	-5.1	28, -6, -16
Right Angular Gyrus	271	-6.6	50, -70, 30
Left Calcarine Gyrus	456	-5.6	-10, -74, 16
Right Calcarine Gyrus	325	-5.3	22, -98, 0
Left Cerebellum IV/V	366	-5.7	-26, -42, -22
Right Cerebellum IV/V	399	-5.2	28, -34, -24
Left Cerebellum VI	913	-5.5	-30, -44, -24
Right Cerebellum VI	872	-5.3	30, -74, -18
Left Cerebellum Crus I	72	-4.9	-42, -64, -22
Right Cerebellum Crus I	196	-4.8	48, -66, -20
Left Middle Cingulate	249	-5.3	-6, 20, 34
Right Middle Cingulate	327	-5.3	8, 26, 34
Left Posterior Cingulate	150	-5	-8, -54, 32
Left Cuneus	144	-6.5	-2, -70, 26
Right Cuneus	233	-4.9	14, -92, 14
Left Inferior Frontal (Operculum)	156	-5.5	-50, 8, 28
Right Inferior Frontal (Operculum)	246	-5.3	48, 8, 28
Left Inferior Frontal (Orbital)	217	-5.8	-30, 36, -12
Right Inferior Frontal (Orbital)	159	-5.4	50, 46, -10
Left Inferior Frontal (Triangular)	274	-5.4	-42, 36, 24
Right Inferior Frontal (Triangular)	108	-5.1	46, 22, 0
Left Medial Frontal (Orbital)	567	-6.7	-10, 50, -6
Right Medial Frontal (Orbital)	445	-6.7	2, 48, -12
Left Middle Frontal	930	-6.3	-42, 42, 26
Right Middle Frontal	317	-5.7	32, 56, -12
Left Superior Frontal	855	-6.8	-22, 60, 6

Description	Cluster Size (# Voxels)	t-value max	MNI coordinate (x, y, z)
Right Superior Frontal	380	-5.7	18, 44, 34
Left Medial Frontal (Superior)	561	-6.2	-8, 50, 18
Right Medial Frontal (Superior)	596	-6.7	8, 58, 6
Left Fusiform Gyrus	960	-7.5	-26, -36, -18
Right Fusiform Gyrus	1038	-5.5	30, -74, -16
Left Heschl Gyrus	93	-5.7	-38, -22, 4
Right Heschl Gyurs	124	-5.6	54, -4, 4
Left Hippocampus	345	-5.7	-26, -10, -18
Right Hippocampus	251	-5.3	22, -8, -20
Left Insula	932	-6.3	-36, -14, 16
Right Insula	975	-6.7	34, 16, 4
Left Lingual Gyrus	710	-6.7	-16, -56, -8
Right Lingual Gyrus	156	-5.3	2, -72, 2
Left Nucleus Accumbens	133	-5.7	-2, 6, -8
Left Inferior Occipital	129	-5.8	-48, -60, -18
Right Inferior Occipital	60	-4.9	48, -62, -14
Right Middle Occipital	418	-6.5	50, -70, 28
Right Superior Occipital	267	-5.5	30, -74, 40
Left Orbitofrontal Gyrus (anterior)	231	-6.1	-38, 40, -18
Right Orbitofrontal Gyrus (anterior)	237	-5.5	32, 48, -14
Left Orbitofrontal Gyrus (lateral)	133	-6.9	-38, 40, -16
Left Orbitofrontal Gyrus (medial)	279	-5.6	-20, 30, -24
Right Orbitofrontal Gyrus (medial)	259	-6.2	16, 22, -20
Left Orbitofrontal Gyrus (posterior)	330	-6.3	-22, 8, -22
Right Orbitofrontal Gyrus (posterior)	194	-5.6	26, 12, -20
Left Olfactory Gyrus	215	-6.3	-2, 6, -10
Right Olfactory Gyrus	166	-5.9	2, 22, -14
Left Parahippocampus	365	-6.4	-22, 8, -24
Right Parahiippocampus	528	-5.4	22, -8, -32
Left Postcentral Gyrus	578	-6.4	-46, -18, 40
Right Postcentral Gyrus	194	-5	56, -6, 38
Left Precentral Gyrus	389	-6.2	-52, -6, 28
Right Precentral Gyrus	508	-6	50, -10, 42
Left Precuneus	462	-6.4	-8, -54, 34
Right Precuneus	461	-5.8	8, -68, 32
Right Putamen	104	-5	30, 14, 4
Left Rectus Gyrus	626	-7.3	-2, 28, -18
Right Rectus Gyrus	544	-6.4	2, 34, -20
Left Rolandic Operculum	373	-6	-38, -16, 16
Right Rolandic Operculum	370	-6.7	52, 6, -2
Left Supramarginal Gyrus	92	-5.1	-44, -36, 24
Right Supramarginal Gyrus	187	-5.2	58, -26, 18

Description	Cluster Size (# Voxels)	t-value max	MNI coordinate (x, y, z)
Left Inferior Temporal Gyrus	977	-6.1	-48, -58, -18
Right Inferior Temporal Gyrus	1238	-6.4	54, 4, -34
Left Middle Temporal Gyrus	1092	-7.1	-50, 4, -32
Right Middle Temporal Gyrus	1462	-7.1	62, -30, -2
Left Middle Temporal Pole	344	-7.8	-46, 10, -28
Right Middle Temporal Pole	604	-6.6	42, 14, -32
Left Superior Temporal Pole	639	-6.1	-22, 6, -22
Right Superior Temporal Pole	489	-6.6	42, 12, -30
Left Superior Temporal Gyrus	810	-6.6	-44, -36, 20
Right Superior Temporal Gyrus	874	-6.1	62, -32, 2
Cerebellum Vermis VIII	101	-4.2	6, -66, -36
Left Middle Occipital	388	-6	-30, -94, 8
Left Superior Occipital	170	-5.1	-20, -92, 24
Left Paracentral Lobule	141	-5.2	-14, -26, 76

Author Manuscript

Author Manuscript

Author Manuscript

Author Manuscript